Continuity of Mitochondrial Budding: Insights from BS-C-1 Cells by *in-situ* Cryo-Electron Tomography

Judy Z Hu[1,2], Lijun Qiao[2], Xianhai Zhao[2], Chang-Jun Liu[2], Guo-Bin Hu[3*]

[1]InSTAR Program, Ward Melville high School, 380 Old Town Rd., East Setauket, NY 11733, USA

[2]Biology Department, Brookhaven National Laboratory, Upton, NY 11973, USA

[3]The Laboratory for Biomolecular Structures, Brookhaven National Laboratory, Upton, NY 11973, USA. ghu@bnl.gov.

*Corresponding author. Email: ghu@bnl.gov

Abstract

Mitochondrial division is a fundamental biological process as it is critical to cellular functionality and vitality. Following up our previous study in HeLa cells, we employed *in-situ* Cryo-Electron Tomography (Cryo-ET) to visualize mitochondrial budding in intact healthy monkey kidney cells (BS-C-1 cells). Our findings reaffirm single and multiple mitochondrial budding, supporting the hypothesis of mitochondrial division by budding. The budding regions vary significantly in diameter which may represent different stages of budding. Notably, rings, ring-like structures, or ER wrapping were not or rarely presented in the budding regions suggesting mitochondrial budding is independent from Drp1 and ER. Furthermore, we uncovered direct interactions between mitochondria and large vesicles, distinct from small mitochondrial-derived vesicles and extracellular mitovesicles. We propose these interacting vesicles may have mitochondrial origins as the extracellular mitovesicles.

Introduction

Mitochondrion are considered the power plants for eukaryotic cells[1]. They are also related to many diseases such as cancer[2] and Alzheimer's disease[3]. Mitochondria are produced by mitochondrial division. Mitochondrial division, thus, determines the life and death of eukaryotic cells and are related to cancer and Alzheimer's disease. Based on previous studies, scientists believe that mitochondria divide by Drp1- and ER-mediated fission[4]. A more recent Cryo-ET study suggests that actin and septin filaments are involved in the mitochondrial fission[5]. As well known, previous studies relied heavily on the visualization

by conventional imaging techniques, such as fluorescence microscopy and conventional electron microscopy. However, even the latest fluorescence microscopy imaging technique is limited by the spatial resolution to ~100 nm[6] which is insufficient to distinguish mitochondrial division that involves contacts of 10-30 nm spacing[7]. Moreover, fluorescence microscopy relies on labeling. In order to visualize a target, researchers need to label the target, which means we can only label and view what we know thus may prevent us from seeing unknown things. Conventional electron microscopy provides higher resolution but suffers artifacts in specimen preparation, including chemical fixation, dehydration, heavy metal staining, which could have resulted in ambiguous or misleading data. *In-situ* Cryo-ET is an emerging technique that provides visualization of cellular structures and cellular processes in artifacts-free and labeling-free conditions with resolutions better than 10nm[8], sufficient for distinguishing mitochondrial division. We previously applied it to the visualization of mitochondria in frozen hydrated intact HeLa cells. And we obtained unprecedented structural data that led to a new hypothesis for mitochondrial division which is that mitochondria divide by budding[9]. The question is whether the data observed in HeLa cells was HeLa specific, as HeLa cells are cancer cells, or general in other cell types. In present study, we carried out the investigation in monkey kidney cells (BS-C-1) which are healthy animal cells. Our results represent a general form or mode for mitochondrial division.

Results and Discussion

Visualization of mitochondria and mitochondrial dynamics, such as mitochondrial division, has been a challenging task. For *in-situ* Cryo-ET imaging of cellular structures, it is important to prepare thin enough specimen. With intact animal cells grown on electron microscopic grids, the cells need to have considerable flat and thin periphery regions. Fig. 1 shows a small area of specimen we prepared in this study. It is on a 200-mesh gold grid coated with Quantifoil holy carbon film on which BS-C-1 cells were grown. The metal meshes are made of gold because gold is not toxic to cells. Quantifoil holy carbon film is the most common supporting substrate for Cryo-EM that cells can grow on. Meanwhile, holes on the carbon film help with blotting during grid freezing. The dark blobs (blue arrows) shown in the grid squares are the cells. Animal cells are usually too thick for electron microscope beam to penetrate which is why they look dark. Nevertheless, the growing edges or peripheries of the cells are flat and thin (green arrow) which are suitable for electron microscopy imaging. Data in this paper was acquired from thin cellular regions like the one pointed by the green arrow.

In *in-situ* Cryo-EM/ET, searching and locating targets for data collection is critical for data collection. A common approach for target search is to use correlative microscopy in which the targets were labeled with fluorescence signals. In this study, we used images of intermediate magnification as shown in Fig.2 for target search. The image shown in Fig.2 was taken from one of the cell peripheries shown in green boxes in Fig.1. Mitochondria and mitochondrial budding features such as narrow connections (yellow arrows) between mitochondria can be clearly visualized which makes it possible to specify targets.

Traditionally, mitochondria were observed in bean-like shapes which is how mitochondria named. Lately, scientists observed more complicated mitochondrial shapes and mitochondrial network suggests the complexity of mitochondrial structures and functions. Compared to visualization by fluorescence microscopy which can show only limited structures that are labeled[6], *in-situ* Cryo-ET displays everything

in the cellular area imaged as shown in Fig.3, such as mitochondrial double membrane, mitochondrial cristae, and dark granules inside mitochondria, ER, microtubes (MT), and vesicles (Vs).

Beside individual mitochondria, mitochondrial budding features were observed not only with single budding shown in Fig.4 but also multiple budding shown in Fig.5. Many images do not show the entire mitochondria bodies because of the camera's size limit. The budding features are very similar to what we observed in HeLa cells. And they also resemble the budding bacteria[12] which belong to the same family in the phylogenetic free as mitochondria[13]. Budding mitochondria may eventually form a mitochondrial network if daughter mitochondria do not split from mother mitochondria and the budding processing keeps going on. Structures of multiple mitochondrial budding as shown in Fig.5 have never been reported before. They may represent simultaneous budding of multiple daughter mitochondria or sequential budding of multiple mitochondria from the same mother mitochodnrion[9]. Clearly, most of the mitochondrial budding sites observed by *in-situ* Cryo-ET are usually quite long and do not present ER wrapping [9,14] or ring-like structures, suggesting neither ER nor DRP-1 is required for mitochondrial budding. It may also suggest Drp1- and ER-mediated mitochondrial fragmentation is a different process from what we observed.

The narrow connecting mitochondrial structures may extend to several hundred nanometers as previously observed by super-resolution microscopy visualization[15] and Cryo-ET[9]. The diameter of narrow regions is usually about 50 nm, consistent with previous Cryo-ET results[9], but contrast to 100 nm by fluorescence microscopy[15].The discrepancy may be due to the accuracy of two imaging techniques.

Mitochondrial derived small vesicles were reported in previous studies[16]. Extracellular mitovesicles were also observed in the study of Down syndrome[17]. Intra- and extracellular vesicles were abundant in *in-situ* Cryo-ET images as shown in Fig.7A pointed by white arrows. Interestingly, we observed direct interaction/contacts of mitochondria and vesicles as shown in Fig.7B-E. These vesicles differ significantly from previously reported small mitochondrial derived vesicle by size, e.g., over 500 nm in this study vs. 70-100 nm in previous study[16]. They also differ from the extracellular mitovesicles[17] because they are intracellular. The meaning of these large vesicles that directly interact with mitochondria requires further investigation. Our preliminary hypothesis is that they originate from mitochondria.

Conclusion

The large scale of mitochondrial budding structures, including single mitochondrial budding and multiple mitochondrial budding, observed in this study confirms previous study in HeLa cells and provides solid evidence to support that mitochondrion budding is the general mode for mitochondrial division. This study shows clearly that mitochondrial budding does not require Drp1 or ER since no Drp1 ring or consistent ER wrapping is presented at the budding sites/regions. It indicates the Drp1- and ER-mediated mitochondrial dynamics, if confirmed by Cryo-ET, is a different processing from mitochondrial budding. Further investigation is required to identify the key molecular factor(s) that regulates mitochondrial budding.

Meanwhile, we observed direct connections/contacts of mitochondria and large vesicles for the first time. The large vesicles differ significantly from previous reported small mitochondrial-derived vesicles in size

and from extracellular mitovesciles by their locations. Nevertheless, we hypothesize that those large vesicles have mitochondrial origins.

Materials and Methods

Specimen Preparation

BS-C-1 cells were acquired from ATCC (www.atcc.org) and cultured according to the ATCC protocol, i.e., in growth media of Eagle's Minimum Essential Medium (EMEM, ATCC) supplemented with 10% Fetal Bovine Serum (FBS, ATCC), and at 37 °C with 5% CO_2. 200 mesh R1/4 or R2/4 Quantifoil holy carbon gold grids (Quantifoil®, Grossloebichau/Jena Germany). were glow discharged in Pelco easiGlow (Ted Pella, USA) with 25 mA current and 20 seconds duration before sterilization by UV light for 15 minutes on each side in a cell culture hood. Sterilized grids were placed in cell culture petri dish (Corning, Corning, NY, USA) containing complete cell growth media and incubated in the cell culture incubator at 37 °C with 5% CO_2 for at least 15 minutes before BS-C-1 cells were introduced into the cell culture petri dish. EM grids on which cells grew to the confluence of 50% or above but below 100% were plunge-frozen with a Lecia EM GP2 plunge freezer. EM grids were blotted for 8 seconds on the back side to minimize the disturbance of the cells when freezing. Frozen grids were stored in the liquid nitrogen storage tank until Cryo-EM examination.

Data Acquisition

Frozen EM grids were imaged on a ThermoScientific Titan Krios G3i Cryo-TEM operated at 300kV and at liquid nitrogen temperature. Tomography images were filtered with a BioQuantum energy filter and acquired with a Gatan K3 Direct Electron Detector and (Gatan, Pleasanton, CA, USA) using Thermo Scientific Tomography program at the nominal magnification of either 33,000x with tilt range of -/+ 48 degree and 3 degree increment or 19,500x with tilt range of +/-50 degree and 2 degree increment, constant dose of 3 electrons on each tilt angle for +/-48 tilt range and 2.5 electrons on each tilt angle for +/-50 degree tilt range. The defocus was set to -5 µm for both tilt schemes.

Image Processing

The tomography tilt series were aligned and reconstructed using fiducial mark-free alignment program AreTomo[10]. All 3D reconstructions were denoised and filtered by nonlinear anisotropic diffusion in IMOD[11]. Visualization was also run in IMOD.

Acknowledgement

This project was sponsored by the Brookhaven National Laboratory's High School Summer Research Program. The work was supported by the DOE, Office of Science, Office of Basic Energy Sciences, especially the Physical Biosciences program of the Chemical Sciences, Geosciences and Biosciences Division under contract no. DE-SC0012704 (to C-JL). Specimen preparation, including cell culture and cell freezing, was performed using the Bioimaging facility at the NSLS-II of BNL. Data was collected at

the Laboratory for Biomolecular Structures of BNL which is supported by the DOE Office of Biological and Environment Research (KP1607011).

Author contribution

GH and CL conceived the research. GH designed the experiments. JH, XZ, JQ, and GH did cell culture. JH and GH prepared Cryo-EM grids, collected and processed data. GH and JH wrote the manuscript. All the co-authors edited the manuscript.

Competing interests

The authors declare no competing financing interests.

References

1. Voet D., Voet J.C., and Pratt C.W. (2006). *Fundamentals of Biochemistry (2nd ed.)*. John Wiley and Cons, Inc. 547-556. ISBN 967-0471214953.
2. Douglas C.W, 2012. Mitochondria and cancer. *Natural Review Cancer* 12: 685-698.
3. Moreira P.I., Carvalho C., Zhu X., Smith M.A., Perry G., 2010. Mitochondrial dysfunction is a trigger of Alzheimer's disease pathophysiology. *Biochemica et Biophysica Acta (BBA) -- Molecular Basis of Disease* 1802:2-10.
4. Rambold A.S., and Lippincott-Schwartz J. (2011). SevERing mitochondria. *Science* 334:186-187.
5. Mageswaran S.K, Grotjahn D.A., Zeng X., et al. (2023). Nanoscale details of mitochondrial constriction revealed by cryoelectron tomography. *Biophysical Journal* 122:3768-3782.
6. Guo Y., Li D., Zhang S., et al., 2018. Visualizing intracellcular organelles and cytoskeleton interactions at nanoscale resolution on millisecond timescales. *Cell* 175:1430-1442.
7. Wu H., Carvlho P., and Voeltz G.K. (2018). Here, there, and everywhere: The importance of ER membrane contact sites. *Science* 361, eaan5835.
8. Turk M. and Baumeister W. (2020). The promise and challenges of Cryo-ET. *FEBS Letters* 594:3243-3261.
9. Hu G.B., 2014, Whole cell Cryo-ET suggests mitochondria divide by budding. *Microscopy and Microanalysis* 20: 1180-1187.
10. Zheng S., Wolff G., Greenan G., et al. (2022). AreTomo: An integrated software package for automated marker-free, motion-corrected cryo-electron tomographic alignment and reconstruction. *Journal of Structural Biology*: X6 100068.
11. Kremer J.R., Mastronarde D., and McIntosh J.R. (1996). Computer visualization of three-dimensional image data using IMOD. *Journal of Structural Biology* 116:71-76.
12. Hirsch P. (1974). Budding bacteria. *Annu Rev Microbiol* 28:391–444.
13. Roger A.J., Munoz-Gomez S.A., and Kamikawa R. (2017). The origin and diversification of mitochondria. *Current Biology* 27:1177-1192.
14. Nedozralova H., Basnet N., Ibiricu I., Bodakuntla S., Biertumpfel C., and Mizuna N. (2022). *In situ* Cryo-electron tomography reveals local cellular machineries for axon branch development. *Journal Cell Biology* 221: e202106086.
15. Shim S.H., Xia C., Zhong G., et el., 2012. Super-resolution fluorescence imaging of organelles in live cells with photoswitchable membrane probes. *Proc Natl Acad Sci USA* 109, 13978–13983.
16. Sugiura A., McLelland G.L., Fon E.A., and McBride H.M., 2014, A new pathway for mitochondrial quality control: mitochondrial-derived vesicles. *The EMBO Journal* 33:2142-2156.
17. D'Acunzo P., Pérez-González, R., Kim Y., et al., 2021. Mitovesicles are a novel population of extracellular vesicles of mitochondrial origin altered in Down syndrome. *Science Advances* 7: eabe5085.

Figure legends

Fig.1 A low magnification (135x) Cryo-EM image of cells grown on electron microscopic grid and directly frozen to liquid nitrogen temperature. Three grid squares marked in green are examples of where cells with thin peripheries (green arrow) that are suitable for high resolution *in-situ* Cryo-EM imaging. There are also empty squares (one example marked in red) where carbon support film broke and got lost during grid handling.

Fig.2 Intermediate magnification (2250x) Cryo-EM image of a cellular region. A lot of mitochondria are presented a few of which are pointed by red arrows . Cristae inside mitochondria can be appreciated. Thin connecting structures (yellow arrows) are visible when zoom in.

Fig.3 2D slices of 3D *in-situ* Cryo-electron tomography reconstruction of individual/independent mitochondria. They are accompanied by but remain some distances from endoplasmic reticulum (ER) . Bars, 200nm.

Fig.4 2D slices of 3D reconstructions showing single mitochondrial budding. A long narrow bridging structure is usually connecting the mother mitochondrion and the daughter mitochondrion. No ring, or ring-like structures, or ER is wrapping the bridging region suggesting the budding is Drp1 and ER-independent. Bars, 200nm.

Fig.5 2D slices of 3D reconstructions showing multiple mitochondrial budding. For the first time, flower like mitochondria are observed. It is quite obvious they represent simultaneous budding or sequential budding from the same mother mitochondria. Bars, 200nm.

Fig.6 Long bridging mitochondrial structures. Several hundred nanometer long connecting structures were observed as in HeLa cells. The diameter of some is about 50 nm but may vary significantly and may develop a new mitochondrion, contrast to the report by previous super-resolution microscopy but consistent with previous Cryo-ET study. Bars, 200nm.

Fig.7 Mitochondria and vesicles. A, Low magnification image show a mitochondria (black arrows) and vesicle (white arrows) rich cellular region. Connections (B, D/E) and membrane fusion (C) between mitochondria and vesicles can be appreciated. (D) and (D) are two 2D slices of the same 3D reconstruction but at different height, they together show a vesicle interacting/associating with a mitochondrion in vertical direction. Bars, 200nm, or otherwise stated.

Fig.1

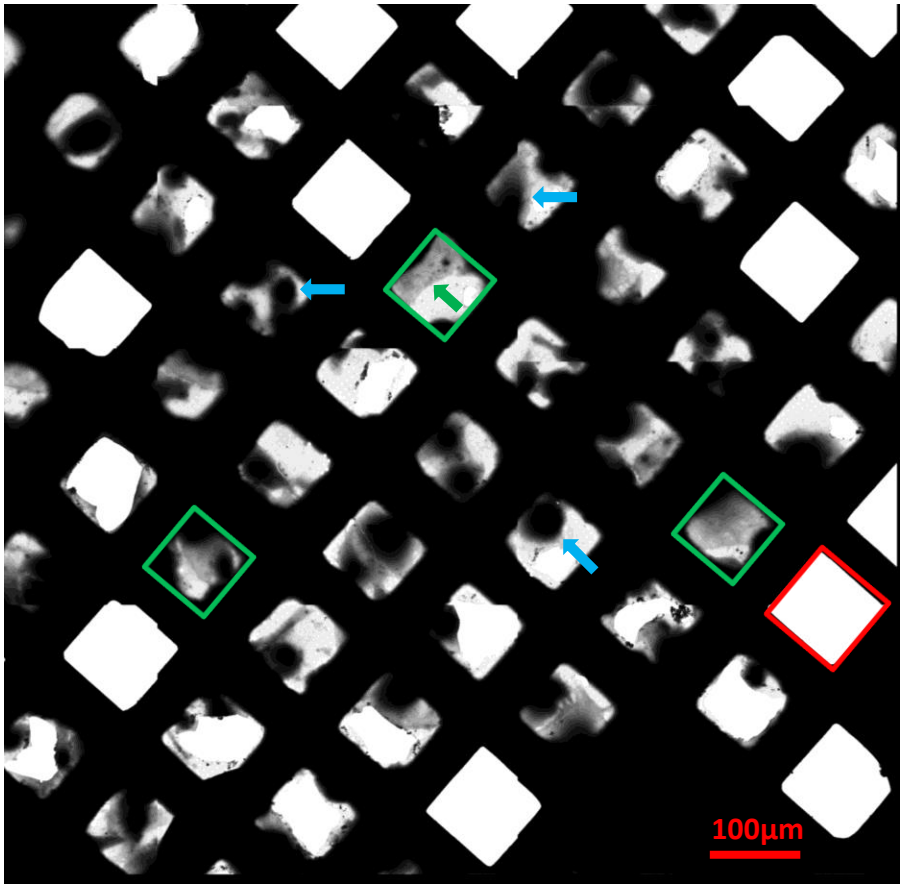

Fig.2

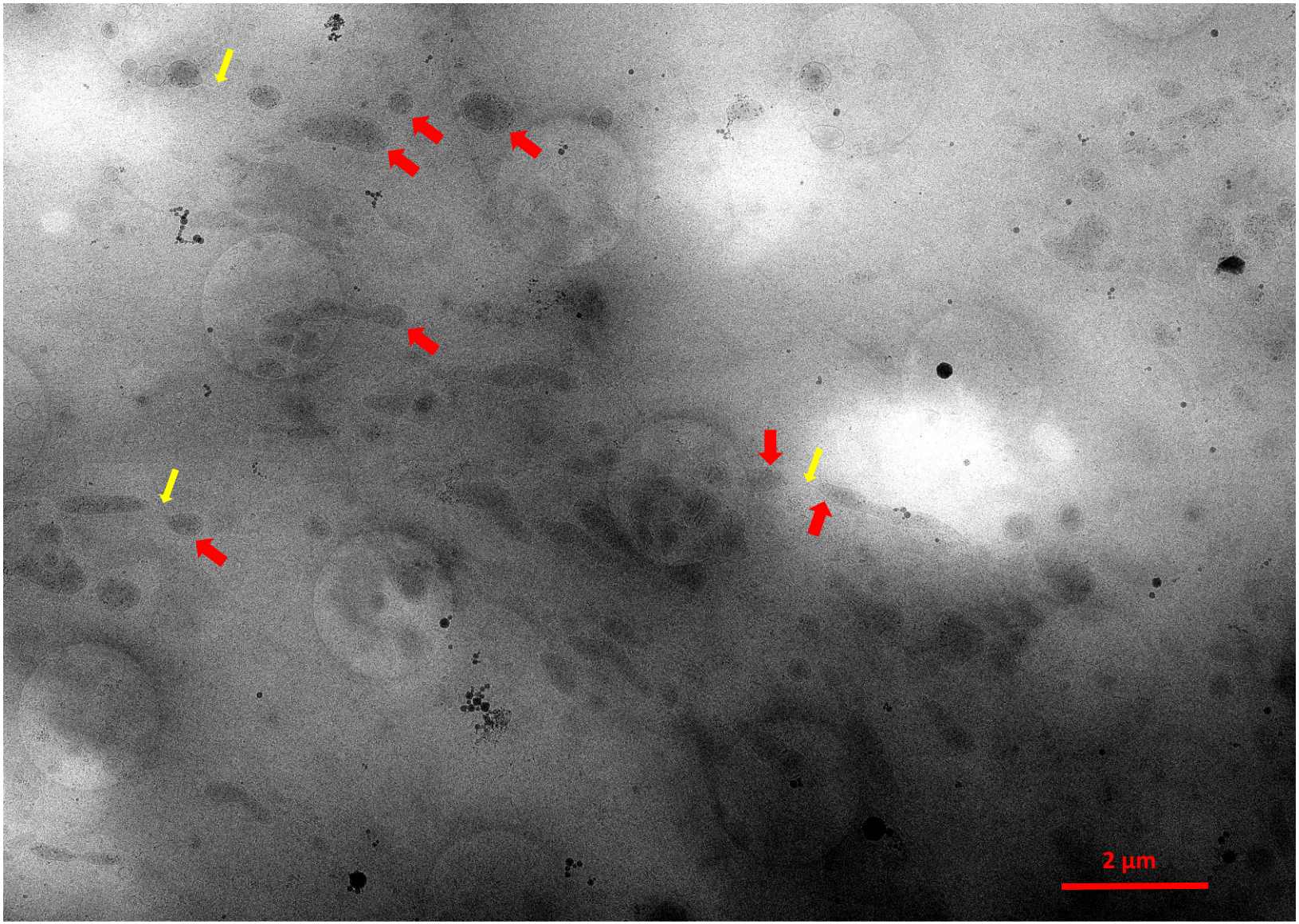

Fig.3

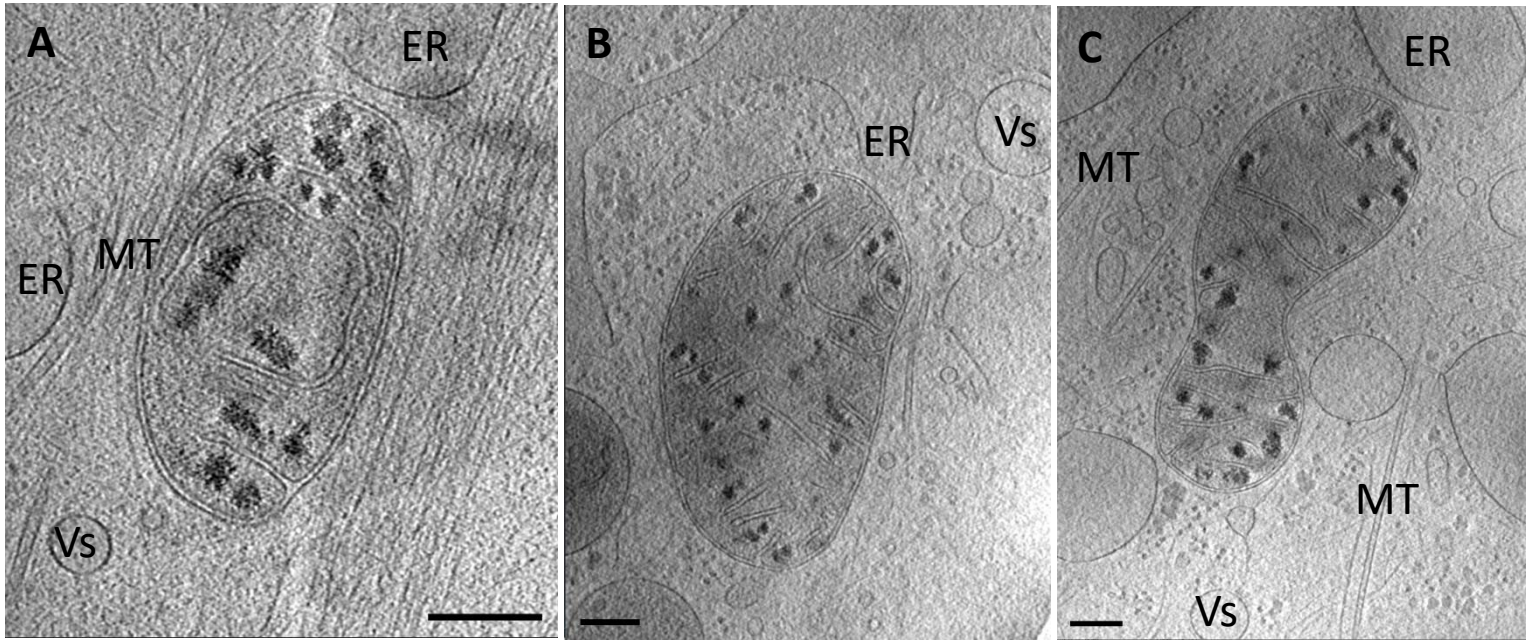

Fig.4,

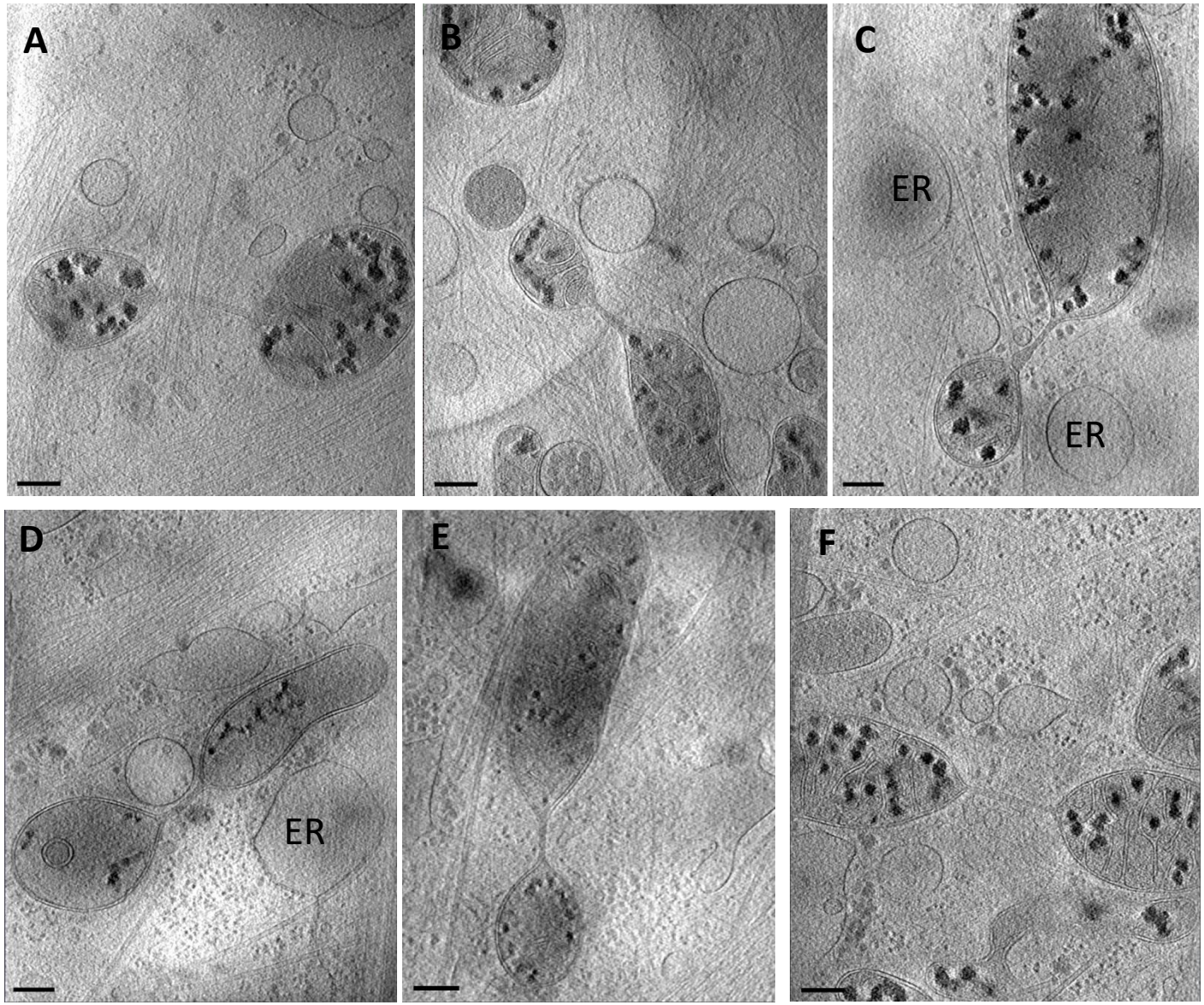

Fig.5

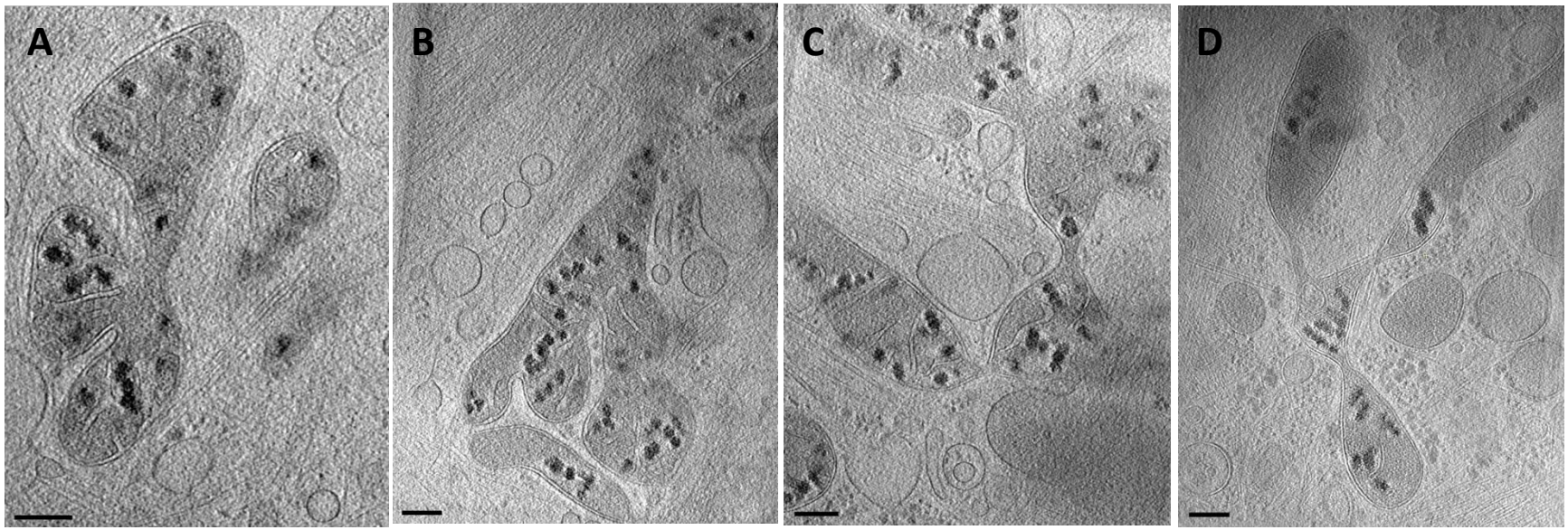

Fig.6

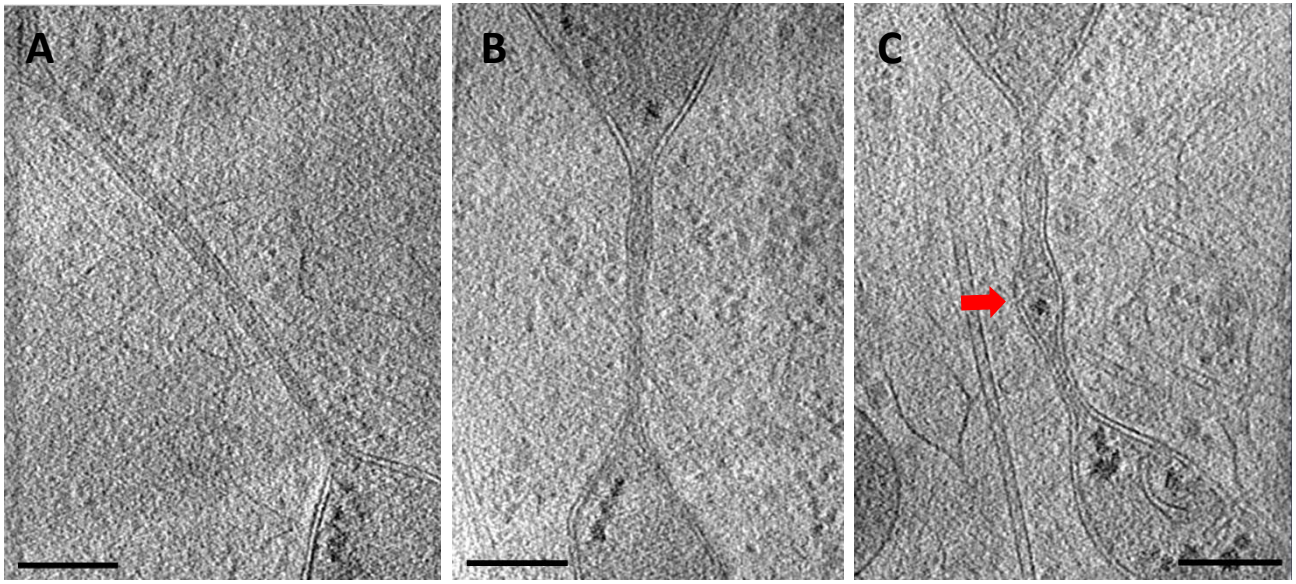
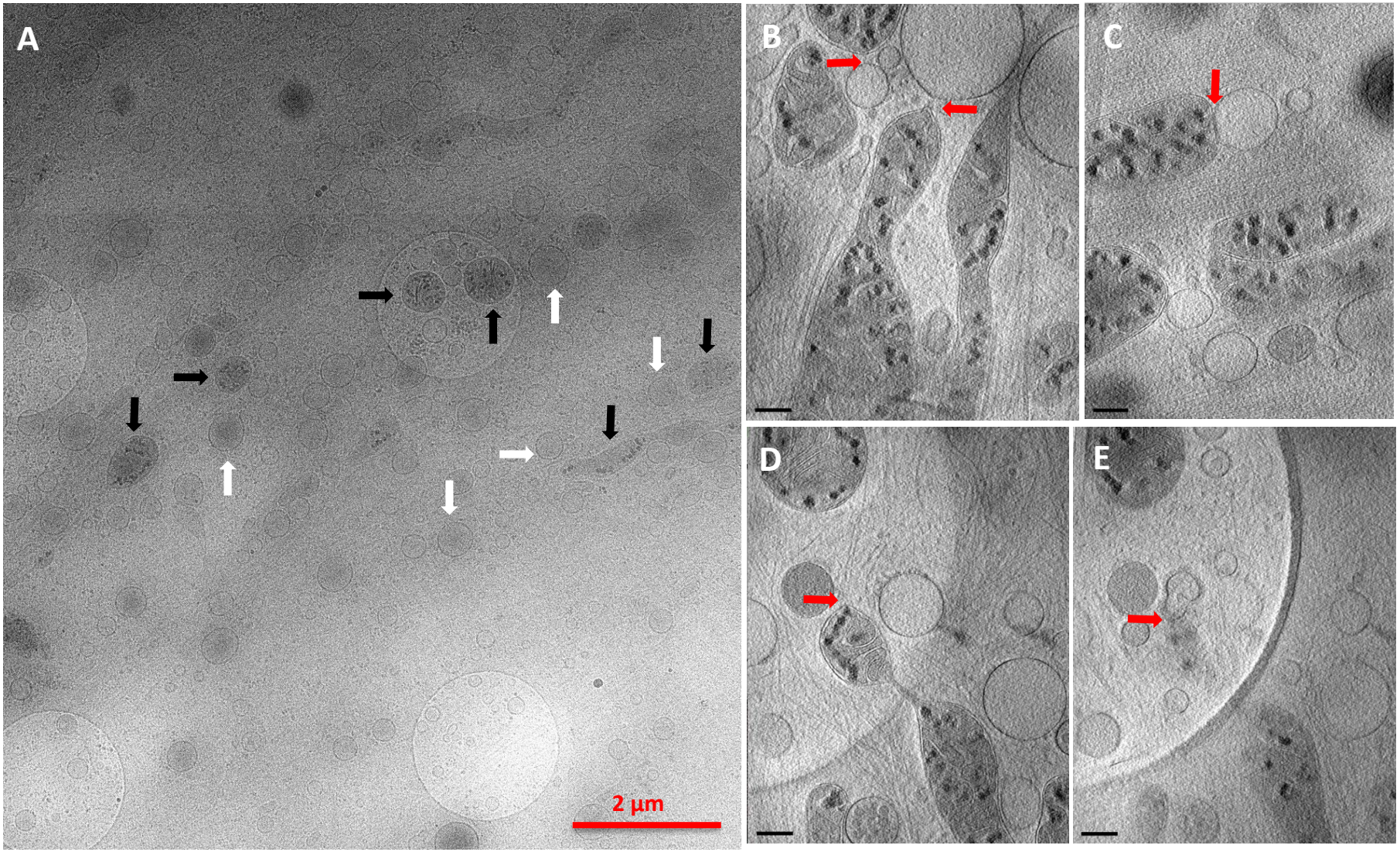
Fig.7